Bull. Mater. Sci., Vol. 3, Number 2, July 1981 pp. 169-184. © Printed in India.

Oxide dielectrics

E C SUBBARAO
Department of Metallurgical Engineering, Indian Institute of Technology, Kanpur 208 016, India

MS received 19 January 1981

Abstract. Three aspects of oxide dielectrics are covered (i) structure engineering: making use of crystal structure and crystal chemistry, the dielectric behaviour can be finely tuned, as illustrated in the systems (Ba, Pb) (Ti, Zr)O_3 and (Ba, Pb) (Ti, Nb)O_3 studied by Biswas. (ii) Defect structure: control of defect structure of Mn-doped $BaTiO_3$ inhibits the reduction of $BaTiO_3$ in reducing atmospheres at high temperatures thus making the use of base metal electrodes possible in manufacturing ceramic capacitors. (iii) Composites: Diphasic composites of oxide dielectrics with other materials may be utilized for producing voltage stable capacitors and dense or flexible piezoelectrics with outstanding properties.

Keywords. Dielectrics; ferroelectrics; defect structure; composites; piezoelectrics.

1. Introduction

Ferroelectrics are an important class of oxide dielectrics. Though the first ferroelectric (Rochelle salt) was discovered nearly sixty years ago, the first oxide ferroelectric ($BaTiO_3$) was found less than forty years ago. These materials possess high dielectric constants (which make them useful in capacitors), high piezoelectric constants (useful in electromechanical transducers) and high pyroelectric coefficients (valuable in thermal sensing). Expanding understanding of the physics and chemistry of the solid state has been applied to systematically develop better oxide dielectrics. Manipulation of structure at various levels—electronic, atomic, micro and macro—has been employed to enhance properties of these materials, sometimes by orders of magnitude. These aspects are examined here with appropriate illustrations.

2. Structure engineering

The most important common feature of oxide ferroelectrics is the existence of oxygen octahedra, which are linked to form a three-dimensional lattice. The octahedra are quite often puckered, lowering the symmetry of the crystal. The extent of puckering is dependent upon the ions located in the cavities formed by the oxygen octahedra. A small, highly charged ion such as Ti, Zr, Nb or Ta is located inside the octahedron in an off-centre position. Oxygen octahedra are linked to give rise to three structure-

types which exhibit ferroelectric behaviour, each of which exhibits polymorphism *e.g.*, perovskite-cubic, tetragonal, orthorhombic, rhombohedral, pyrochlore—cubic, rhombohedral; and tungsten bronze type—orthorhombic, tetragonal (see, for example, Jona and Shirane 1962). Ionic substitutions with size, charge and polarizability of the ions as parameters provide means to finely tune the structure and thereby the properties of these oxide ferroelectrics, which was carried out by Professor A B Biswas in establishing structure maps of the systems $(Ba, Pb)_{1-\delta}$ (Ti, Nb)O_3 and (Ba, Pb) (Ti, Zr)O_3.

2.1 *$(Ba, Pb)_{1-\delta}$ (Ti, Nb)O_3 system*

This system is of significance, since it includes a number of ferroelectric compounds—$BaTiO_3$, $PbTiO_3$ and $PbNb_2O_6$, and extensive ferroelectric solid solutions—(Ba, Pb) TiO_3, (Ba, Pb)Nb_2O_6, etc. For compositions sintered at 1280 - 1300°C in PbO atmosphere for 1 hr, Srikanta *et al* (1962) have established the structure map for this system (figure 1). In this two-dimensional diagram, a point x, y represents the composition $Ba_yPb_{1-y-x/2}$ $Ti_xNb_{1-x}O_3$.

(A) Cubic perovskite arises when the incorporation of Nb for Ti in (Ba, Pb)TiO_3 creates vacancies in the A sites of the ABO_3 lattice and raises the symmetry to cubic. Density and x-ray intensity data confirm the formula as $A_{1-\delta}BO_3$, similar to that of Ba(Ti, Nb)O_3 system (Subbarao and Shirane 1959).

(B) Tetragonal perovskite is stable for compositions with $Nb^{5+} < 0{\cdot}1$, and for compositions with $Nb^{5+} > 0{\cdot}1$ only if the Pb^{2+} content is high. The tetragonal distortion decreases as Pb^{2+} is replaced by Ba^{2+} or Ti^{4+} by Nb^{5+} along line xy in figure 1.

(C) Orthorhombic perovskite region is only approximately fixed in figure 1.

(D) *Cubic pyrochore.* These compositions have the general formula $(Pb, Ba)_{1-\delta}$ (Nb Ti)O_3 with $\delta = 0{\cdot}15$ to $0{\cdot}375$, $Ba^{2+} = 0$ to $0{\cdot}225$ and $Nb^{5+} = 0{\cdot}3$ to $0{\cdot}75$. Density

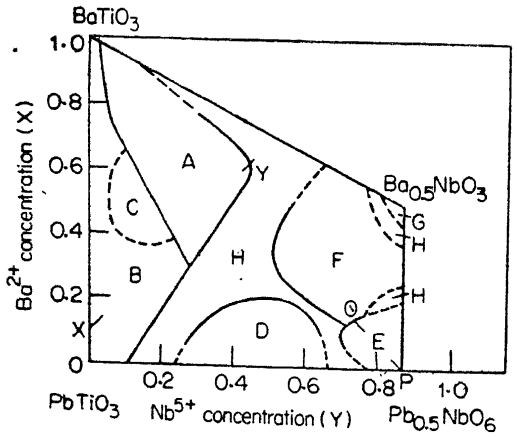

Figure 1. Structure map of $(Ba, Pb)_{1-\delta}$ (Ti, Nb)O_3 system (after Srikanta *et al* 1962). (A) Cubic perovskite phase; (B) Tetragonal $BaTiO_3$ type; (C) Orthorhombic $BaTiO_3$ type; (D) Cubic pyrochore type; (E) Orthorhombic $PbNb_2O_6$ type; (F) Tetragonal $PbNb_2O_6$ type; (G) Orthorhombic $BaNb_2O_6$ type; (H) Mixture phase.

suggest vacancies in the 16(*d*) (occupancy 11·3 to 12·6 out of 16) and oxygen pancy 47·1 to 50·1 out of 56) sites. Thus it may be similar to $Pb_{1.5}Nb_2O_{6.5}$ and Jaffe 1953). The electrical conductivity is quite low and hence mixed cy is not likely for any of the ions.

Orthorhombic tungsten bronze ($PbNb_2O_6$) type. This occurs in the vicinity Nb_2O_6 ($a=17{\cdot}65$, $b=17{\cdot}91$, $c=7{\cdot}736$ Å and $z=20$). The orthorhombic distor-b/a is maximum (1·014) for pure $PbNb_2O_6$ and decreases along the line PO in l as Nb^{5+} and Pb^{2+} are replaced by Ti^{4+} and Ba^{2+} respectively. The crystal ure of the orthorhombic phase is shown in figure 2, which shows the tunnel age sites which are surrounded by five and four oxygen octahedra respectively combe and Lewis 1958). There are 16 tunnel and 8 cage sites in a unit cell, which 20 are filled by Pb^{2+} ions in the case of $PbNb_2O_6$. The larger coordi-n number of tunnel sites and lower repulsive energy of ions in these sites must r the filling of tunnel sites first. It is likely that 4 cage (smaller) sites are vacant. neasured densities suggest that the maximum number of A ions that can be mmodated at the A sites depends on the Pb: Ba ratio. As shown in figure 3, aximum occupancy is 22 for pure lead compounds (point A) and increases with sing Ba content (A to B) up to the maximum permissible value of 24. At still r Ba : Pb ratio, the maximum value of A site occupancy decreases from 24 to ong BC, possibly because the large A ions tend to change the orthorhombic ure to a tetragonal one.

Tetragonal tungsten bronze type. The measured density values indicate 5·1 2, 8·9 to 9·7 and 26·7 to 29·1 ions at the A, B and O sites respectively, on the ption that the ratio of metal-to-oxygen has remained unchanged during sinter-

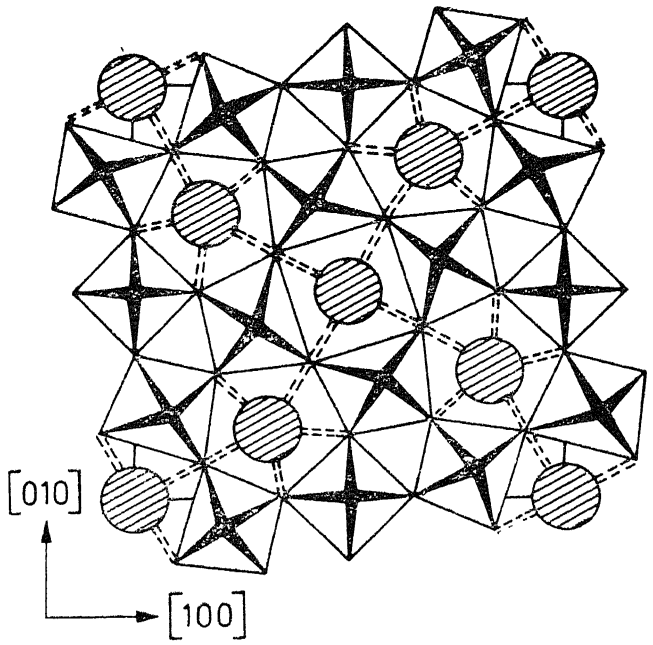

Figure 2. Projection of the structure of tetragonal tungsten bronze ($K_{0{\cdot}57}WO_3$) or paraelectric Pb, Nb_2O_6 parallel to [001]. K^+ or Pb^{2+} ions (circles) are located ($Z=0$) in 'tunnels'– or 'cages' formed by WO_6 or NbO_6 octahedra ($Z=\pm\frac{1}{2}$).

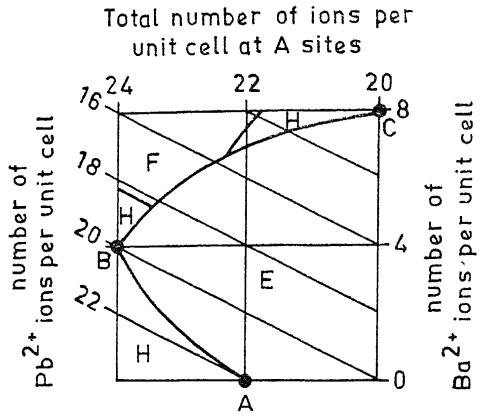

Figure 3. Occupancy of tunnel and cage sites in orthorhombic tungsten bronze structure with varying Ba/Pb ratio (after Srikanta *et al* 1962).
(E) $PbNb_2O_6$ Orthorhombic; (F) $PbNb_2O_6$ tetragonal; (H) Mixture.

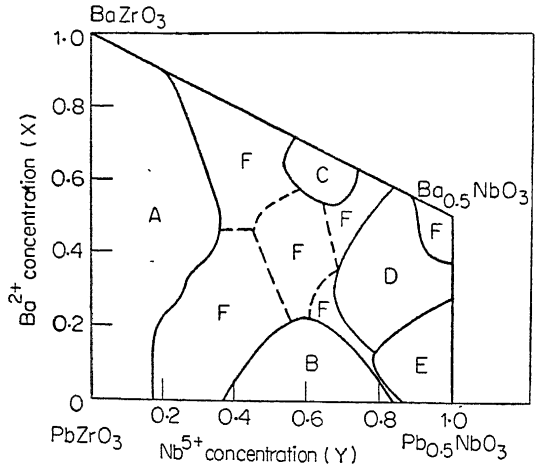

Figure 4. Structure map of (Ba, Pb) (Nb, Zr)O_3 system (after Chincholkar *et al* 1969).
(A) Cubic perovskite phase; (B) Cubic pyrochlore type; (C) Tetragonal $PbTiO_3$ type; (D) Tetragonal tungsten bronze type; (E) Orthorhombic $PbNb_2O_6$ type; (F) Mixture phase.

(G) Barium niobate phase is stable in a narrow region near the orthorhombic $BaNb_2O_6$ phase ($a=12{\cdot}17$, $b=10{\cdot}25$ and $c=3{\cdot}94$ Å) (Francombe 1960).

(H) Two-phase regions separate the four structure types (perovskite, tungsten bronze, pyrochlore, $BaNb_2O_6$) from each other.

2.2 *(Ba, Pb) (Nb, Zr)O_3 system*

A two-dimensional constitution diagram for this system is shown in figure 4, where a point (x, y) represents the composition $Ba_xPb_{1-x-y/2}\ Nb_yZr_{1-y}O_3$ (Chincholkar *et al* 1969).

(A) Cubic perovskite exists in the Zr-rich portion. The lattice parameter a increases linearly with Ba^{2+}/Nb^{5+} ratio due to the differences in ionic radii. Density and x-ray intensity data suggest that these compositions have vacancies in the A sites, as in Ba (Ti, Nb)O_3 system (Subbarao and Shirane 1959).

(B) Cubic pyrochlore exists in the Pb-rich compositions and can be indexed on the basis of $A_2B_2O_7$ compounds. Density and x-ray intensities suggest vacancies in the A and oxygen sites, as in $Pb_{1.5}Nb_2O_{6.5}$ (Cook and Jaffe 1953).

(C) Tetragonal $PbTiO_3$ type occurs in the narrow composition range of Ba^{2+} (0·55-0·70) and Nb^{5+}(0·55-0·70). A study of the dielectric properties of these compositions (Chincholkar *et al* 1970) shows that the Curie temperature (T_c) decreases with increasing c/a (figure 5). At fixed Nb^{5+} concentration, the c/a values were reported to increase with increasing Ba^{2+} concentration, possibly due to the larger size of Ba^{2+} (1·43Å) than that of Pb^{2+} (1·32 Å) and are larger than that for $PbTiO_3$ for many compositions. Since the polarizability of Ba^{2+} (74·8 $Å^3$) is lower than that of Pb^{2+} (89·5$Å^3$), it is expected that a decrease in T_c should occur with increasing Ba^{2+} concentration (and increasing c/a). One observes a linear decrease in T_c with decreasing average polarizability of A site (Ba+Pb) ions at fixed Nb^{5+} concentration) (figure 5).

(D) Tetragonal tungsten bronze type, similar to tetragonal $PbNb_2O_6$ ($a=b=12·46$ and $c=3·907$ Å), occurs in the Nb^{5+} rich region. Density data suggest vacancies in the B and oxygen sites.

(E) Orthorhombic tungsten bronze type occurs near the $PbNb_2O_6$ corner of the diagram. The orthorhombic distortion b/a and $V^{1/3}$ decrease with decreasing

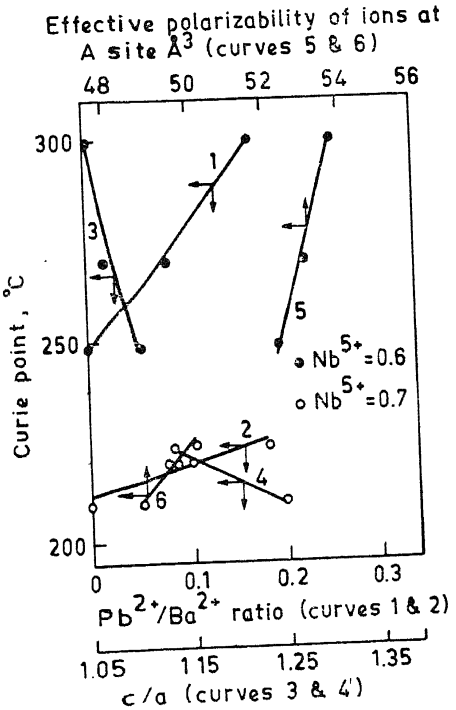

Figure 5. Variation of Curie temperature of tetragonal $PbTiO_3$ type phase as a function of c/a ratio, Pb/Ba ratio and average polarizability of A site ions (Chincholkar *et al* 1970).

Pb^{2+}/Ba^{2+} ratio when Nb^{5+} content is kept constant at 0·90, similar to that in the (Ba, Pb)Nb_2O_6 solid solutions. At $Ba^{2+} > 0.2$, the lattice becomes that of tetragonal tungsten bronze type for $Nb^{5+} = 0{\cdot}90$.

(F) Mixed phases are observed between the various structure types—perovskite (cubic and tetragonal), pyrochlore, and tungsten bronze (tetragonal and orthorhombic).

These studies enable one to engineer a desired crystal structure of a given type and symmetry and thereby achieve controlled dielectric properties.

3. Defect structure

3.1 *Introduction*

A multilayer capacitor is made by sintering a stack consisting of alternate layers of ceramic titanate dielectric and electrodes in a single operation. The electrode for this purpose should have a melting point above the sintering temperature (1300-1400°C), be stable under the sintering conditions and not react with the dielectric. Palladium and Pd-Ag alloys are among the few possible electrode materials. The escalating price of these materials prompts the use of the base metal electrodes (*e.g.* Ni), even though these electrodes require sintering in reducing atmospheres. Barium titanate under such conditions becomes highly conducting, due to the conversion of Ti^{4+} ions into Ti^{3+} ions accompanying the formation of oxygen vacancies, according to

$$Ba\overset{4+}{Ti}O_3 \xrightarrow{\textit{reduction}} Ba\overset{4+}{Ti}_{1-2x}\ \overset{3+}{Ti}_{2x}O_{3-x}+\tfrac{x}{2}O_2. \qquad (1)$$

Incorporation of some impurity ions [*e.g.* Mn (Herbert 1963, 1965; Burn 1978, 1979), Ga (Seuter 1974; Daniels 1978), Cr, Mg, Co (Burn and Maher 1975)] was found to prevent or minimize reduction of $BaTiO_3$ under appropriate conditions. Of these, manganese has been reported to be most effective. Recent studies have clarified the role of Mn.

3.2 *Energetics*

The free electrons which arise when $BaTiO_3$ is reduced can be trapped at the positive ion (Ba, Ti or impurity ion at Ba or Ti sites) or negative ion (oxygen or impurity halogen) sites. The site preferred for electron trapping is one which causes maximum decrease of lattice energy (ΔW). Following Mott and Littleton (1938),

$$\Delta W = BE_{M^{m+}} - BE_{M^{n+}} - I_{M^{n+} \rightarrow M^{m+}}, \qquad (2)$$

where BE is the binding energy of the particular ion concerned and I is the ionization potential for the specific case. The potential energy of two ions in the $BaTiO_3$ lattice has been calculated using only the Coulombic term and the ΔW values have been evaluated for various impurity ions, using the above potential energy and standard ionization potentials in equation (2) (table 1) (Desu and Subbarao 1980).